Jurnal Ilmu Fisika
Vol. 14, No. 2, September 2022, pp. 95–107
ISSN: 1979-4657 (Print); 2614-7386 (Online)
https://doi.org/10.25077/jif.14.2.95-107.2022

Jurnal Ilmu Fisika
Open Access

Effects of State Degeneration in 3D Quantum Lenoir Engine Performance

Ade Fahriza[1], Trengginas E. P. Sutantyo[1]
[1]Theoretical Physics Laboratory, Department of Physics, Faculty of Mathematics and Natural Sciences, Universitas Andalas, Limau Manis, Padang, 25163, Indonesia

Article Info

Article History:

Received June 21, 2022
Revised July 02, 2022
Accepted July 03, 2022

Keywords:

quantum lenoir engine
single-particle
cubic potential
degenerate state
efficiency

Corresponding Author:

Trengginas E. P. Sutantyo,
Email:
trengginasekaputra@sci.unand.ac.id

ABSTRACT

We study the performance of the quantum Lenoir engine using single-particle confined within the cubic potential. In 3D potential structure, particles degenerate into multiple states at identic energy level which occurs on the excitation state of the particles. Deliberating the degeneration effects, the confined particle has possibility to produce more energy efficiency as engine's working substance. The particle is able to freely move in three directions of *x*, *y*, and *z*-axis simultaneously, which gives three degrees of freedom to the particle in the cubic potential. By limiting to two eigen states, a basic explanation to the condition of the particle was provided. The efficiency of the 3D quantum Lenoir engine is better than the classical model of the Lenoir engine despite the similarity in the formulation. Moreover, we also consider the efficiency comparison between the 3D model, with some state modifications, and the 1D efficiency of the quantum Lenoir engine. As expected, degeneration of the particle's states plays a role in the enhancement of the quantum Lenoir engine's efficiency. Moreover, we also derived the power output of the 3D quantum Lenoir engine. Thus, this study clearly gives a sight of the performance of quantum Lenoir engine model in the 3D manner.

1. INTRODUCTION

The formalism using mechanical quantum in terms of thermodynamics to achieve a more efficient engine model has been carried out since the 1950s (Scovil & Schulz-DuBois, 1959). Quantum engine study has shown its potential since Bender et al., (2000) discovered the relation between the classical Carnot engine to the quantum modeling Carnot engine. Application of quantum principle in thermodynamical terms gives out clarity on fundamental problems, such as Maxwell's demon and the second law of thermodynamics (Kieu, 2006). Moreover, there have been several researches on the different cases that prove the compatibility of quantum mechanics applications into thermal engine terms (Ali et al., 2020; Belfaqih et al., 2015; Fernández, 2022; Muñoz & Peña, 2012; Singh, 2020; Singh & Rebari, 2020).

Studying quantum engine turns out to be the most potent way to boost the efficiency an engine could reach. By treating the working substance (like free particles) in the quantized state, the engine is able to subdue the time restriction of quasi-static on a reversible engine (Yuan et al., 2022). Theoretically, the particle confined in a cubic potential act according to the environment set up inside the engine. It is due to particles would have a distinguished state on every treatment they receive. For example, if the particle is statistically boson, then it is different from the fermion particle (Akbar et al., 2018; Wang & He, 2012). In the same manner, variating the dimensional of quantum engine model generates different results in the engine properties, like the efficiency of the engine (Latifah & Purwanto, 2013).

The 1-Dimensional explanation is the most basic study of quantum engines as the foundation to prove that quantum can be implied into certain classical model engines. Lenoir engine is one of potentially merged to quantum engines model. Saputra (2021) has proven that the classical and quantum Lenoir engines are both similar in the way of efficiency formulation, but quantum Lenoir engines have higher efficiency because of its specific heat ratio. However, the efficiency of the 1D model is lower compared to 3D quantum engine models. For example, both Sutantyo et al., (2015) and Abdillah & Saputra (2021) studied the comparison between the 1D, 2D, and 3D models of a quantum engines and the 3D models was proved to have higher efficiency due to the state degeneration occurred within the confined particle. Moreover, the 1D and 2D model of quantum engine are only a theory and hard to be implemented into real engine construction.

Between the 1D and 3D model, there is the 2D model which the particle strictly expands into two axes. Based on the research carried out by Abdillah & Saputra (2021), Sutantyo et al. (2015) and Belfaqih et al. (2015), the 2D model has less efficiency than the 3D model but has higher efficiency than the 1D model. The position of the 2D model is exactly between the 1D and 3D model. The previous researches are enough to prove that the efficiency of the 2D model is not be higher than 3D model. Thus, this condition become the consideration of the 2D model being remove from the topic. Its efficiency is not higher than the 3D model, and it is still challenging to be applied in real life.

By studying the 3D model, the closely real performance of the quantum engine efficiency can be showed. Cubic structure is the basic form of a 3-Dimensional model of an engine whose same length is on each side. In 3D model, the particle which acts as working substance is allowed to move in three directions (x, y, and z-axis) which gives the particle more degree of freedom. Single-particle was chosen due to the model needs to expand simultaneously to achieve the degeneration effects. This condition can be simply obtained in single-particle term rather than many particles.

In this paper, we construct the cubic potential model of the quantum Lenoir engine with a confined single-particle which have never been carried out before. The particle changes freely between two states, ground and first excited states. The model expands and compresses simultaneously within the Lenoir cycle. All representation of motion is considered in quantum mechanical view. The efficiency as the result of the formulation is compared to the 1D model of quantum Lenoir engine. In addition, the result is also compared to other degenerate state. Thus, the improvement of the efficiency obtained by the model can be shown, to prove whether the improvement on previous researches of other 3D engines is also occurred in Lenoir engine 3D model. Moreover, the power output of the engine is also considered as the possible performance of the 3D quantum Lenoir engine.

2. METHOD

2.1 3D Quantum Heat Engine

For the 3D case, the free particle acts as a working substance and is established in a symmetry cubic potential in which infinite potential (potential barrier) exists at L point of the cubic. This particle only be allowed to move freely between the ground state (as the initial state) and the first excitation state (as the final state). We sought this quantum system by considering the 3D model of time-independent Schrödinger equations

$$-\frac{\hbar^2}{2m}\nabla^2\phi(\mathbf{r})+V(\mathbf{r})\phi(\mathbf{r})=E\phi(\mathbf{r}), \tag{1}$$

where $\varphi(\mathbf{r})$ refers to eigenfunction of the particle as function of three axes (x, y, z) with E as the average energy within the system, while the potential environment, $V(\mathbf{r})$, of the system ought to be infinite in this model. By deriving Equation (1) to the three axes, we obtained the eigenfunction as the solution of particle wave-motion

$$\varphi(x,y,z)=\sqrt{\frac{8}{L^3}}\sin\left(\frac{n_x\pi x}{L}\right)\sin\left(\frac{n_y\pi y}{L}\right)\sin\left(\frac{n_z\pi z}{L}\right), \tag{2}$$

which n_x, n_y and n_z represented the quantized properties of the wave function. Furthermore, we also obtained the Hamiltonian as the total energy of the system as (Zettili, 2009),

$$E_{n_x n_y n_z} = \frac{\pi^2 \hbar^2}{2mL^2}\left(n_x^2 + n_y^2 + n_z^2\right), \tag{3}$$

where the ground state ($n_x = n_y = n_z = 1$) of this quantum system shows the first condition or initial condition of the particle inside the cubic is

$$E_1 = \frac{3\pi^2 \hbar^2}{2mL^2}. \tag{4}$$

The force exerted by the particle to each side of the moving wall of the cubic is the derivation of consisting energy by the change of the cubic in each axis, written as

$$F_i = -\frac{dE}{dL_i}. \tag{5}$$

Since the volume changes simultaneously ($dL_x = dL_y = dL_z = dL$) (Sutantyo, 2020), the initial force (**F**) of the particle is

$$\mathbf{F} = F_x + F_y + F_z = -3\frac{dE}{dL}. \tag{6}$$

The mechanical work done can be obtained by deriving the Equation (5)

$$W = \int \mathbf{F} dL = \int \left(F_x + F_y + F_z\right) dL. \tag{7}$$

Since the force **F** in each three different axes has the same value ($F_x = F_y = F_z$), the total mechanical work done by the particle can be written as

$$W = 3\int F_x dL, \tag{8}$$

which "3" will be later known as the degree of freedom of the confined particle.

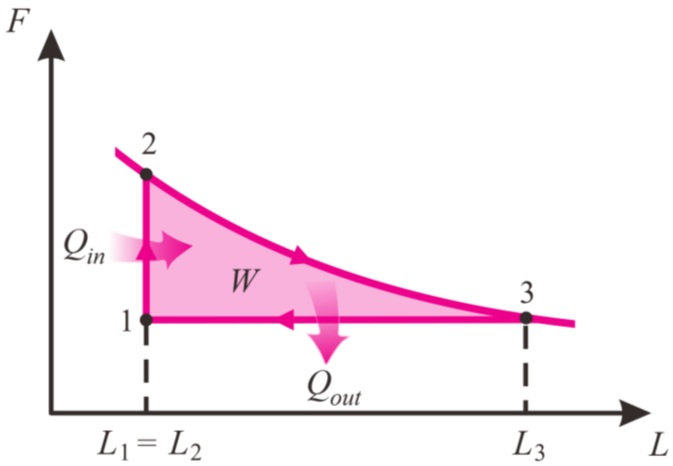

Figure 1. The Three-Process of quantum Lenoir cycle with, (1 → 2) isovolume, (2 → 3) isentropic expansion, and (3 → 1) isobaric compression (Sutantyo et al., 2021).

2.2 Quantum Thermodynamics Lenoir Cycle

Lenoir cycle is constructed only on 3-process of a cycle, i.e., isovolume, isentropic, and isobaric as shown in Figure 1. Therefore, the Lenoir engine is unique. It can run at a higher cycle speed than the

4-process standard engine. The Lenoir cycle starts with the isovolume thermodynamic process. The volume of the system remains constant ($L_2 = L_1$). During this process, the state of the particle is a linear combination of its ground state excites and the first excited state. These conditions, as illustrated in Figure 2, are represented as follow

$$\Psi_{isovolume} = a_{111}\varphi_{111} + a_{211}\varphi_{211} + a_{121}\varphi_{121} + a_{112}\varphi_{112}, \tag{9}$$

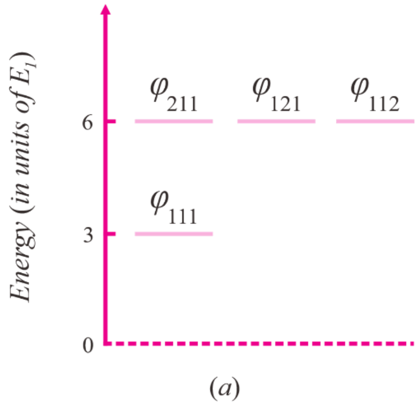

$E_{n_x n_y n_z}/E_1$	$n_x n_y n_z$	g_n
6	(211), (121), (112)	3
3	(111)	1

(b)

Figure 2. (*a*) The first two state of 3D quantum system with (*b*) energy levels and the degeneracies for the cubic potential, with $E_1 = \pi^2\hbar^2/2mL^2$ (Zettili, 2009).

where Ψ and a refers to the wave function and the probability of the particle in the quantum system, respectively. Within the process, from the initial state to the final state, the particle ought to move freely in each axis to reach its final state without changing the volume of the cubic potential. As a result, the energy of the system can be written as

$$E_{isovolume} = \frac{\pi^2\hbar^2}{2mL^2}\left(6 - 3a_{111}^2\right), \tag{10}$$

with L in Equation (10) equals to L in Equation (4) due to the volume constancy in this process. At the end of isovolume process, the particle is in a fully excited condition where $a_{111}^2 = 0$ with the volume remains at L_1. Thus, the excited energy is written as

$$E_{211} = \frac{6\pi^2\hbar^2}{2mL_1^2}, \tag{11}$$

which the energy is split equally due to the degenerate state of the particle ($E_{211} = E_{121} = E_{112}$) (Sutantyo et al., 2015). Thus, the total energy gained in this process is

$$E_2 = E_{211} + E_{121} + E_{112} = 3\frac{6\pi^2\hbar^2}{2mL_1^2}, \tag{12}$$

where the "3" in Equation (12) indicates the particle's degree of freedom because of the degeneration. Since the volume of cubic potential remains constant, the work done in this process also remains zero, $W_{isovolume} = 0$. Based on the first law of thermodynamics, all energy within this process refers to the amount of heat inducted into the system equally between the three axes from the high-energy heat bath,

$$Q_{in} = E_2 - E_1 = \frac{15\pi^2\hbar^2}{2mL_1^2}. \tag{13}$$

As the particle reaches its final state, the cycle continues to isentropic expansion. The system is kept enclosed to the surroundings where heat exchange can not occur, and the state remains constant at the highest state. By this condition, the wave function is

$$\Psi_{isentropic} = a_{211}\varphi_{211} + a_{121}\varphi_{121} + a_{112}\varphi_{112}\,. \tag{14}$$

The energy from the end of the isovolume process was converted as the force of particle to move the wall in amount of work done which can be written as

$$F_{isentropic(X)} = F_{isentropic(Y)} = F_{isentropic(Z)} = \frac{6\pi^2\hbar^2}{mL^3}, \tag{15}$$

and

$$W_{isentropic} = 3\int_{L_2=L_1}^{L_3} F_{isentropic(X)}dL = \frac{9\pi^2\hbar^2}{mL_1^2}\left(1-\frac{L_1^2}{L_3^2}\right), \tag{16}$$

respectively.

At the last stage of the Lenoir cycle, the system is compressed by constant force in the isobaric thermodynamic process. The particle returns to its initial state, and the heat will be deducted to the low-energy sink bath in a condition of

$$\Psi_{isobaric} = a_{111}\varphi_{111} + a_{211}\varphi_{211} + a_{121}\varphi_{121} + a_{112}\varphi_{112}, \tag{17}$$

which the constant force along the process is

$$F_{isobaric(X)} = F_{isobaric(Y)} = F_{isobaric(Z)} = \frac{\pi^2\hbar^2}{mL^3}\left(6-3a_{111}^2\right). \tag{18}$$

The constant force shows a relation between the initial and final condition of the system as

$$\left(\frac{L_3}{L_1}\right)^3 = 2\,, \tag{19}$$

which means, at this state, the cubic potential can only expand as far as $L_3 = L_1\sqrt[3]{2}$. Using Equation (17) where $a_{111}^2 = 1$ with the final volume is L_1 as the constant force, the total mechanical works in this process is

$$W_{isobaric} = 3F_{isobaric(X)}\int_{L_3}^{L_1} dL = \frac{9\pi^2\hbar^2}{mL_1^2}\left(1-\frac{L_3}{L_1}\right). \tag{20}$$

Meanwhile, the change of internal energy within the process can be derived by substracting the initial and final energy of the process, $dU = E_{final} - E_{initial}$. The initial energy correlates with the energy inside the model when the particle is at an excitation state. On the other hand, the final energy represents the energy left after the model interacts with the low-energy sink bath, represented as

$$dU_{isobaric} = \frac{9\pi^2\hbar^2}{2mL_1^2}\left(1-\frac{L_3}{L_1}\right). \tag{21}$$

The change of heat can be derived by substituting Equation (20) and Equation (21) to the first law of thermodynamics,

$$dQ = dU_{isobaric} + W_{isobaric} = \frac{9\pi^2\hbar^2}{2mL_1^2}\left(3-3\frac{L_3}{L_1}\right), \tag{22}$$

as the change of heat represents the total heat expelled to the sink bath. The heat out of the system ought to be written in the negative form to show that this heat flows out of the system to the environment or sink bath in this model,

$$Q_{out} = -\frac{9\pi^2\hbar^2}{2mL_1^2} 3\left(\frac{L_3}{L_1} - 1\right), \tag{23}$$

but the value of the Q_{out} itself should be written in absolute brackets

$$Q_{out} = \left| \frac{9\pi^2\hbar^2}{2mL_1^2} 3\left(\frac{L_3}{L_1} - 1\right) \right|. \tag{24}$$

Total work done within the Lenoir cycle is derived by integrating the mechanical works of the cycle, as follows

$$W_{cycle} = \oint \vec{F} dL = 3\int_{L_2 = L_1}^{L_3} F_{isentropic(X)} dL + 3F_{isobaric(X)} \int_{L_3}^{L_1} dL = \frac{9\pi^2\hbar^2}{2mL_1^2}\left(\frac{L_3^3}{L_1^3} - 3\frac{L_3}{L_1} + 2\right), \tag{25}$$

where the mechanical work in the isovolume process is zero due to the volume change does not occur. The mechanical work in a Lenoir cycle of Equation (25) can be expressed as

$$W_{cycle} = \frac{9\pi^2\hbar^2}{2mL_1^2}\left(\alpha^3 - 3\alpha + 2\right), \tag{26}$$

where $\alpha = L_3 / L_1$ is the compression ratio of the potential cubic volume. The total mechanical work is considered on three directional works, which means it already has the component of its degree of freedom if we look back at Equations (16) and (20). While the thermal efficiency of the engine is

$$\eta_{3D} = \frac{W_{cycle}}{Q_{in}} = 1 - \frac{9}{5}\frac{(\alpha - 1)}{(\alpha^3 - 1)}. \tag{27}$$

Similar to the works, the inducted energy is also considered in a degenerated way. Thus, Equation (27) shows that the efficiency of the quantum Lenoir engines in 3D observation is higher than its 1D model, whose efficiency (Saputra, 2021) of

$$\eta_{1D} = 1 - 3\frac{(\alpha - 1)}{(\alpha^3 - 1)}. \tag{28}$$

The quantum Lenoir engines efficiency in Equation (28) can be generally expressed as

$$\eta_{1D} = 1 - \gamma, \tag{29}$$

where $\gamma = 3(\alpha - 1) / (\alpha^3 - 1)$ from the general formulation of the comparison between input and output heat, Q_{out}/Q_{in}, of the quantum Lenoir engine. In the same way, the 3D model's efficiency is

$$\eta_{3D} = 1 - \frac{3}{5}\gamma, \tag{30}$$

which the value of γ is decreasing as the value of α gets higher in the range of $0 < \gamma \le 0.78$ if $1 < \alpha^3 \le 2$.

2.3 Power of the 3D Quantum Lenoir Engine

The power output, P, done by the quantum engines is the derivation of the relation between the total work done within the cycle and the total time of one cycle, τ, which can be written as

$$P = \frac{W_{cycle}}{\tau}. \tag{31}$$

The value of τ is obtained by

$$\tau = \frac{L_{total}}{\bar{v}} , \quad (32)$$

where L_{total} is the total length change within one cycle, while $\bar{v}$ is the average velocity of the length to change (Saputra, 2021; Sutantyo et al., 2021). Since the 3D model is a cubic potential that expands and compresses simultaneously, the value of L_{total} on each axis should be the same

$$L_{total_{(x)}} = L_{total_{(y)}} = L_{total_{(z)}} = L_{total} , \quad (33)$$

which L_{total} can be obtained as follow

$$L_{total} = \Delta L_{isovolume} + \Delta L_{isentropic} - \Delta L_{isobaric} , \quad (34)$$

with the isobaric compression process is expressed in negative sign. Moreover, the 3D model moves simultaneously which means the total time needed by the engine is identical,

$$\tau_x = \tau_y = \tau_z = \tau . \quad (35)$$

In the same idea, the average velocity of the cycle expansion is

$$\bar{v}_x = \bar{v}_y = \bar{v}_z = \bar{v} . \quad (36)$$

Under the condition of Equation (33), (35) and (36), the derivation of the power output of the quantum engine 3D model can be inspected only in one axis as

$$\tau_x = \frac{L_{total_{(x)}}}{\bar{v}_x} , \quad (37)$$

in which the derivation of Equation (37) already represents all three axes.

According to Equation (34), the total change of volume is

$$L_{total_{(x)}} = \left(L_2 - L_1\right)_x + \left(L_3 - L_2\right)_x - \left(L_1 - L_3\right)_x . \quad (38)$$

Since the volume L_1 and L_2 are equal, then

$$L_{total_{(x)}} = 2\left(L_3 - L_1\right) . \quad (39)$$

By inputting Equation (39) to Equation (37), we obtained the estimated time of one cycle for the quantum Lenoir engine in simultaneously condition as

$$\tau_x = \frac{2\left(L_3 - L_1\right)_x}{\bar{v}_x} , \quad (40)$$

or in general,

$$\tau = \frac{2\left(L_3 - L_1\right)}{\bar{v}} . \quad (41)$$

Therefore, the power output is derived by inputting the Equation (26) and (41) to Equation (31), as follow

$$P = \frac{9\pi^2\hbar^2}{2mL_1^2}\bar{v}\frac{\left(\frac{L_3^3}{L_1^3} - 3\frac{L_3}{L_1} + 2\right)}{2\left(L_3 - L_1\right)} = \frac{9\pi^2\hbar^2}{4mL_1^2}\bar{v}\frac{\left(\alpha^3 - 3\alpha + 2\right)}{\left(\alpha - 1\right)} . \quad (42)$$

The power formulation of Equation (42) should be reduced to dimensionless formulation to show the correlations between power and the compression ratio and the efficiency of the engine, as follow

$$P^* = \frac{P}{K} = \frac{\dfrac{9\pi^2\hbar^2}{4mL_1^2}\bar{v}\dfrac{\left(\alpha^3 - 3\alpha + 2\right)}{\left(\alpha - 1\right)}}{\dfrac{\pi^2\hbar^2}{4mL_1^2}\bar{v}} = 9\frac{\left(\alpha^3 - 3\alpha + 2\right)}{\left(\alpha - 1\right)} = 9\chi , \tag{43}$$

where $K = \pi^2\hbar^2\bar{v}/4mL_1^2$ is a constant that reduces the power formulation to dimensionless power form, while $\chi = (\alpha^3 - 3\alpha + 2) / (\alpha - 1)$ is the general power of the quantum Lenoir engines.

2.4 Degenerate States Comparison

The engine's efficiency in the other forms of the state degenerations can be derived in the same way as the methods above. The result of derivation can be seen in Table 1 below.

Table 1 Various state degenerations comparison, with $W_{1D} = [\pi^2\hbar^2 (\alpha^3 - 3\alpha + 2)] / 2mL_1^2$

Model	States	Energy Level	Efficiency	Mechanical Work	Dimensionless Power
1D	–	$\frac{3\pi^2\hbar^2}{2mL^2}$	$1-\gamma$	W_{1D}	χ
3D$^{(A)}$	(211) (121) (112)	$\frac{6\pi^2\hbar^2}{2mL^2}$	$1-\frac{3}{5}\gamma$	$9W_{1D}$	9χ
3D$^{(B)}$	(221) (122) (212)	$\frac{9\pi^2\hbar^2}{2mL^2}$	$1-\frac{3}{4}\gamma$	$9W_{1D}$	9χ
3D$^{(C)}$	(311) (131) (113)	$\frac{11\pi^2\hbar^2}{2mL^2}$	$1-\frac{4}{5}\gamma$	$9W_{1D}$	9χ
3D$^{(D)}$	(222)	$\frac{12\pi^2\hbar^2}{2mL^2}$	$1-\gamma$	$3W_{1D}$	3χ

Table 1 indicates the comparison of the performance that is shown by the highest energy level, the efficiency, the general formulation of the efficiency, and the dimensionless power for each different state. Based on the energy level, the state (222) is the state that produces the highest energy level. Meanwhile, the state (211)(121)(112) is the most efficient model. The efficiency of the state (222) is similar to the 1D model because the degeneration of the particle is fallen, but the power of the state (222) is higher than the 1D model and it can be clearly seen that the mechanical works are different. Nevertheless, all powers of the degenerate states, 3D$^{(A)}$, 3D$^{(B)}$, and 3D$^{(C)}$, are identic despite the efficiency differences.

3. RESULTS AND DISCUSSION

Both Equation (27) and (28) show a similarity in formulation which means the only factors that differs 3D and 1D model of quantum Lenoir engine are the degree of freedom the particle possess and efficiency gradient which is clearly seen in Equation (29) and (30). Degeneration of the particle state is the main role of this occurrence. In the 1D model, the particle strictly only moves in one directional way. In contrast, the 3D model has three different ways to move, which means the particle becomes freer to produce works. Thus, the engine becomes more efficient as compared, $\eta_{3D} > \eta_{1D}$.

According to previous researches, Sutantyo et al., (2015) studied the efficiency of quantum Carnot engine using single-particle confined to cubic potential 3D and they proved that the simultaneously expand to achieve degenerated state can easily be obtained if observed under single-particle confined in cubic potential. The illustration of the state degeneration is shown at the isentropic expansion of the engine which has been visualized in Figure 3. The wave function on Equation (13) signifies the condition of a degenerated particle in the cubic potential. As its an isolated condition, the internal energy only depends on the state of the particle. The particle would divide the energy to push the potential wall in three directions.

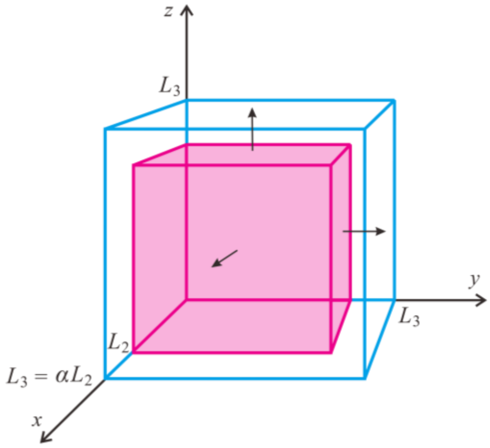

Figure 3. Isentropic expansion of the cubic potential in degenerate state of the particle

The 1D model which has been carried out by Saputra (2021), the quantum Lenoir engines have higher efficiency than the classical Lenoir engines due to the value of its specific heat ratio. In their research, the particle in which is the working substance in their engine model is only able to expand at the *x*-axis. This condition signifies the straightforward and essential explanations about the correlation between quantum and thermodynamics within Lenoir cycle. However, unlike the 3D model, the 1D model cannot be applied into real life and the efficiency is lesser than the 3D model due to the degeneration effects cannot occur in the 1D model.

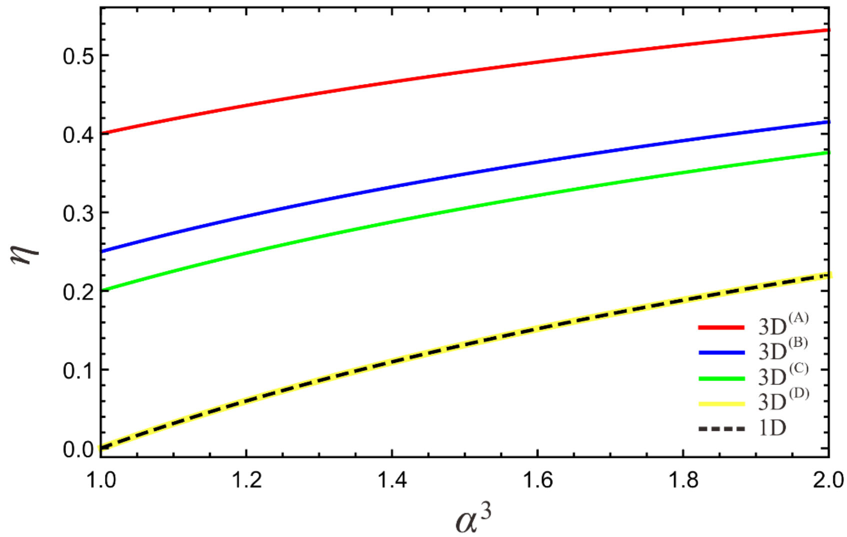

Figure 4. Efficiency vs. Compression Ratio. The compression ratio, α, on Equation (19) of the lowest state degeneration, (211)(121)(112), is used to obtain general comparison of the performance of the quantum Lenoir engine models.

Figure 4 is the visualization of comparison between efficiency that proves the efficiency of the engine in 3D model is much higher than 1D as the compression ratio, α, goes increased. Moreover, the graph shows that the $3D^{(A)}$ is the highest efficiency model. Efficiency of an engine is measured by how much inducted and ejected energy within the engines cycle. Since the $3D^{(A)}$ has only one excited state particle, the engine has fully ejected the energy at low compression ratio, $\alpha^3 = 2$. That is why the $3D^{(A)}$ model is more efficient than the other degenerate models even though the three degenerate states have similar heat out value. This means that the 3D model of degenerated particles of quantum Lenoir engine is explicitly independent to the number of degenerations, g_n, but highly depends on the maximum compression ratio for each model which also related to the energy level of the particle. This condition also occurred in the model of Brayton and Otto engine in the research by Akbar et al., (2018) and Latifah & Purwanto (2013).

Meanwhile, the $3D^{(D)}$ model in (222) state has similar efficiency with the 1D model which is literally lower than the degenerated states. After the particle is fully excited to the (222) state, the degenerate states that particles possess before is fallen. This fallen gives impact to the decreasing of the total amount of heat inducted and ejected from the engine. Therefore, the efficiency somewhat becomes similar to the 1D model of the quantum Lenoir engines as seen in Table 1. In a higher compression ratio, the efficiency from the models are closely the same because in a long distance of expansion, the engine performs quasi-static condition at constant speed of particle. This condition only occurred on two eigen states of the particle in the cubic. At higher state, the particle would consist of more degenerate states but also there are completeness reduction which mean there should be more consideration to the condition of the particle as said in the research carried out by Sutantyo (2020).

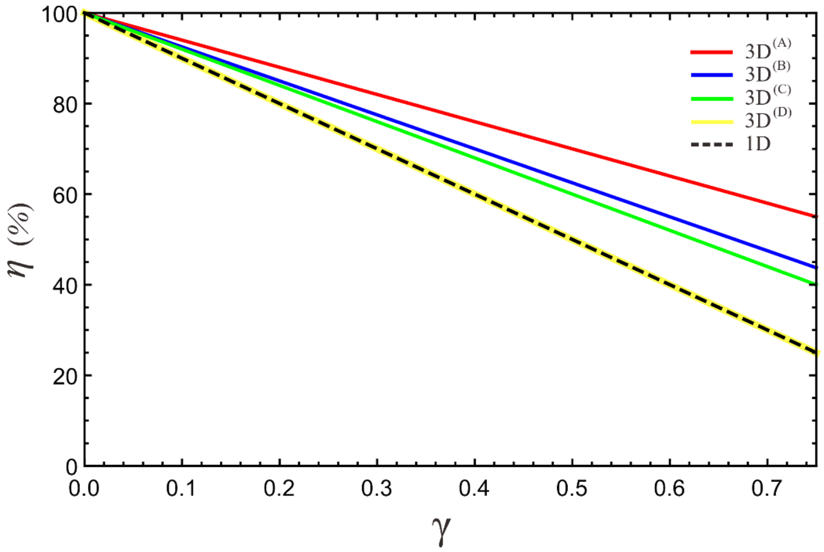

Figure 5. Percentage of Efficiency vs. Gamma, with $0 < \gamma \leq 0.75$.

The performance of the quantum Lenoir engine in term of efficiency can be seen in Figure 5. At the furthest expansion of the $3D^{(A)}$ states, the efficiency reaches approximately 55%. While the 1D model and the $3D^{(D)}$ model only reaches around 25%. The increasement of the degeneration is clearly shown in this way that about 30% increasement to the efficiency is reached. Whereas the other degenerated states are only between the $3D^{(A)}$ and the 1D model, but the increasements of efficiency are also occurred this way.

To calculate the power of the engine, we need to derive the time needed for one cycle as seen in Equation (37). In the simultaneously 3D structure observation, we found that the cubic potential expands at the same time for each axis. It means that the time needed for one cycle is equal on each axis observed as written in Equation (33), (35) and (36). Therefore, the only factors that differs the power output of an engine produce is the amount of the mechanical work done within the process which can be seen in Table 1. The $3D^{(D)}$ model which has identic efficiency to the 1D model produces more power due to the mechanical works done by this state is higher than the 1D model. Compared to the 1D model mechanical work, the degenerate state, $3D^{(A)}$, $3D^{(B)}$, and $3D^{(C)}$, in Table 1 produce about 9 times larger than the 1D model. Since the total time cycle is the same, the power produced is also 9 times larger.

Figure 6 shows that as the compression ratio goes higher, the graph becomes steeper. Meanwhile the 1D and the $3D^{(D)}$ model is less steep. This means in high compression ratio, the power produced by the engine is become higher as the particle degenerate more. As referred to the graph, it is impossible the 1D and 3D$^{(D)}$ model to reach the same or even higher power output than the degenerate state. Its dues to in those models the particle are only consist one state, while the degenerate state has three distinguished state. This means that the power of the 3D quantum Lenoir engine model is independent to the level of the state it has, but only depend on the number of the degeneration occurred. This condition is also occurred in Singh (2020) research of the 1D quantum Brayton engine using non-interacting fermion particles as working substance. The distinguishing of the particle state shows that power critically depends on the number of the particle within or in this 3D degenerate model is the number of the degenerate state.

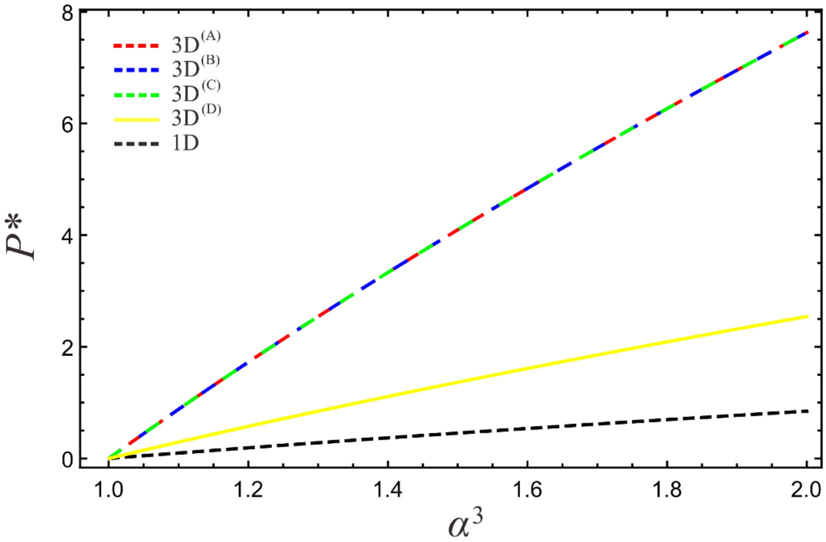

Figure 6. Dimensionless Power vs. Compression Ratio

Comparing the power and efficiency in Table 1, the 3D$^{(A)}$ model in states (211)(121)(112) is outnumbered the other model in both performance. Based on the Figure 7 where the *x*-axis is the efficiency and the *y*-axis is the dimensionless power, the 3D$^{(A)}$ starts at 0.4 efficiency with the power also becomes higher as the compression is increased. In the same way, the 3D$^{(B)}$ and 3D$^{(C)}$ models also have steep increasement both power and efficiency. In opposite, the 1D and 3D$^{(D)}$ have less steep plot due to the increasement of the power is not significant as the compression ratio goes higher, but the 3D model still has the higher power despite the similarity of the efficiency value.

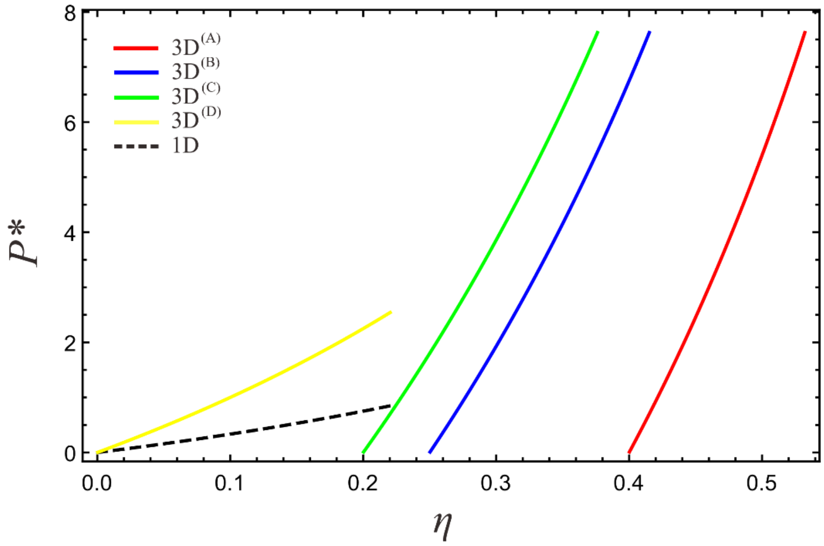

Figure 7. Dimensionless Power vs. Efficiency.

4. CONCLUSION

The result has shown that performance of quantum Lenoir engine is significantly improving in the 3D model rather than its 1D model. Especially the $3D^{(A)}$ model that both efficiency and power is the best compared to the other model. The other $3D^{(B)}$ and $3D^{(C)}$ models have the same power output with the $3D^{(A)}$ model, but the efficiency is rather lower. In other hand, the 1D and $3D^{(D)}$ model have a similarity in the value of the efficiency, but the power is absolutely different which means the $3D^{(D)}$ model is better than the 1D model due to the power comparison. The degenerate state is fallen in the $3D^{(D)}$ model due to the completeness reduction. Thus, the $3D^{(D)}$ model is not better than the degenerated models due to the efficiency depends on the particle state and energy level. Moreover, the power of the engine model is highly related to the number of states of the particle whereas the degeneration has more state than the $3D^{(D)}$ model. The 3D quantum Lenoir engine model can be realized by occupying the quantum dot as the working substance of the quantum engines in future research Moreover, the question of how higher particles states with more degeneration and completeness affect the performance of the engine is also needed to be a valuable consideration in our next research.

ACKNOWLEDGEMENT

This work was financially supported by Universitas Andalas with research grant No. T/38/UN.16.17/PT.01.03/IS-RDP/2021.

REFERENCE

Abdillah, F., & Saputra, Y. D. (2021). Quantum-Mechanical Brayton Engine based on a Boson Particle Inside Cubic Potential. *Journal of Physics: Conference Series*, *1726*(1).

Akbar, M. S., Latifah, E., & Wisodo, H. (2018). Limit of Relativistic Quantum Brayton Engine of Massless Boson Trapped 1 Dimensional Potential Well. *Journal of Physics: Conference Series*, *1093*(1).

Ali, Md. M., Huang, W.-M., & Zhang, W.-M. (2020). Quantum thermodynamics of single particle systems. *Scientific Reports*, *10*(1), 13500.

Belfaqih, I. H., Sutantyo, T. E. P., Prayitno, T. B., & Sulaksono, A. (2015). Quantum-Carnot engine for particle confined to 2D symmetric potential well. *AIP Conference Proceedings*, *1677*.

Bender, C. M., Brody, D. C., & Meister, B. K. (2000). Quantum mechanical Carnot engine. *Journal of Physics A: Mathematical and General*, *33*(24), 4427–4436.

Fernández, J. J. (2022). Optimization of energy production in two-qubit heat engines using the ecological function. *Quantum Science and Technology*, *7*(3), 035002.

Kieu, T. D. (2006). Quantum heat engines, the second law and Maxwell's daemon. *The European Physical Journal D*, *39*(1), 115–128.

Latifah, E., & Purwanto, A. (2013). Quantum Heat Engines; Multiple-State 1D Box System. *Journal of Modern Physics*, *04*(08), 1091–1098.

Muñoz, E., & Peña, F. J. (2012). Quantum heat engine in the relativistic limit: The case of a Dirac particle. *Physical Review E*, *86*, 061108.

Saputra, Y. D. (2021). Quantum Lenoir Engine with a Multiple-eigenstates Particle in 1D Potential Box. *Journal of Physics: Conference Series*, *1726*(1).

Scovil, H. E. D., & Schulz-DuBois, E. O. (1959). Three-Level Masers as Heat Engines. *Physical Review Letters*, *2*(6), 262–263.

Singh, S. (2020). Quantum Brayton Engine of Non-Interacting Fermions in a One Dimensional Box. *International Journal of Theoretical Physics*, *59*(9), 2889–2900.

Singh, S., & Rebari, S. (2020). Multi-level quantum diesel engine of non-interacting fermions in a one-dimensional box. *The European Physical Journal B*, *93*(8), 150.

Sutantyo, T. E. P. (2020). Three-State Quantum Heat Engine Based on Carnot Cycle. *Jurnal Fisika Unand*, *9*(1), 142–149.

Sutantyo, T. E. P., Belfaqih, I. H., & Prayitno, T. B. (2015). Quantum-Carnot engine for particle confined to cubic potential. *AIP Conference Proceedings*, *1677*.

Sutantyo, T. E. P., Fahriza, A., & Abdullah, Z. (2021). Optimizations of Multilevel Quantum Heat Engine with N Noninteracting Fermions Based on Lenoir Cycle. *arXiv*:2112.02904v2 [cond-mat. stat-mech].

Wang, J., & He, J. (2012). Optimization on a three-level heat engine working with two noninteracting fermions in a one-dimensional box trap. *Journal of Applied Physics*, *111*(4).

Yuan, H., Ma, Y.-H., & Sun, C. P. (2022). Optimizing thermodynamic cycles with two finite-sized reservoirs. *Physical Review E*, *105*(2), L022101.

Zettili, N. (2009). *Quantum Mechanics: concepts and applications* (2nd ed.). John Wiley & Sons, Ltd.